

Nonlinear control of a 20-story steel building with active piezoelectric friction dampers

Chaoqiang Chen[†] and Genda Chen[‡]

*Department of Civil Engineering, University of Missouri-Rolla, 111 Butler-Carlton Hall,
Rolla, MO 65409-0030, U.S.A.*

(Received January 25, 2001, Accepted April 29, 2002)

Abstract. A control algorithm combining viscous and non-linear Reid damping mechanisms has been recently proposed by the authors to command active friction dampers. In this paper, friction dampers and the proposed algorithm are applied to control the seismic responses of a nonlinear 20-story building. Piezoelectric stack actuators are used to implement the control algorithm. The capacity of each damper is determined by the practical size of piezoelectric actuators and the availability of power supply. The saturation effect of the actuators on the building responses is investigated. To minimize the peak story drift ratio or floor acceleration of the building structure, a practical sequential procedure is developed to sub-optimally place the dampers on various floors. The effectiveness of active friction dampers and the efficiency of the proposed sequential procedure are verified by subjecting the building structure to four earthquakes of various intensities. The performance of 80 dampers and 137 dampers installed on the structure is evaluated according to 5 criteria. Numerical simulations indicated that the proposed control algorithm effectively reduces the seismic responses of the uncontrolled 20-story building, such as inelastic deformation. The sub-optimal placement of dampers based on peak acceleration outperforms that based on peak drift ratio for structures subjected to near-fault ground motions. Saturation of piezoelectric actuators has adverse effect on floor acceleration.

Key words: active control; piezoelectric friction damper; steel moment resisting frame; inelastic responses; control algorithm; seismic performance; near-fault effect.

1. Introduction

Building structures are often exposed to multiple hazards including extreme windstorms and strong earthquakes. Structural damages under such environmental loads can not only cause economic losses, but also pose a real threat to life. Structural control provides a viable means to protect building structures from such damages. Several types of friction dampers have been proposed for building structures under earthquake excitations (Yang *et al.* 1994, Kannan *et al.* 1995, Inaudi 1997). They have very salient features such as low operating energy and guaranteed dissipation of energy by friction and therefore do not cause instability of the structure being controlled.

Piezoelectric materials can generate a significant amount of stress when exposed to an electric

[†] Ph.D Candidate

[‡] Associate Professor

field and subjected to constraint on their deformation due to strong electromechanical coupling of the material. Piezoelectric actuators can quickly and accurately respond to a driven command such as voltage signal. They offer such unique features as effectiveness over wide frequency bands, high-speed actuation, low power consumption, simplicity, reliability, and compactness as demanded in civil engineering applications (Housner *et al.* 1994, Kamada *et al.* 1998).

Recently the authors proposed the use of piezoelectric friction dampers in mitigating the maximum responses of elastic buildings under dynamic loads (Chen *et al.* 2000a, Chen *et al.* 2000b). Four piezoelectric actuators were used to regulate the clamping force applied on the sliding surfaces of a friction damper. A new control algorithm, which combines viscous and non-linear Reid damping mechanisms, has been developed to command friction dampers. It has been demonstrated very effective in suppressing the harmonic responses of single-story structures. In this paper, the proposed algorithm and friction dampers are further studied to control multi-story inelastic buildings under earthquake loading.

The benchmark control problem (Ohtori *et al.* 2000) for a seismically excited nonlinear 20-story building is considered in this investigation. The size of dampers and their capacity are first estimated based on the state of practice in the fabrication of piezoelectric actuators and the availability of high voltage power supplies. The sensors (LVDT), control devices (dampers), and digital controller (algorithm) are then designed and implemented in numerical simulation for the full-scale building in MATLAB. It is followed by the placement of piezoelectric friction dampers on various floors of the building. A practical sequential procedure is developed to sub-optimally place the dampers on the building structure with the peak drift ratio or peak acceleration of the structure as optimization objective. Finally, the potential saturation effect of actuators on the seismic performance of dampers is addressed.

2. Piezoelectric friction damper (PFD) and control algorithm

Consider a friction damper as schematically shown in Fig. 1. It consists of two U -shaped bodies, one sliding against the other. The contact force, $N(t)$, acting on the sliding surfaces is controllable. The friction damper generates a dissipative force proportional to the contact force and the coefficient of friction between the two bodies. By adjusting the contact force based on the feedback of damper slippage, it is possible to improve the dynamic behavior of structures by utilizing the friction dampers. One way to control the contact force is to use piezoelectric stack actuators to generate the required contact force according to certain control logic. The piezoelectric stack actuators proposed here are composed of many thin layers of PZWT100 ceramic material, which are

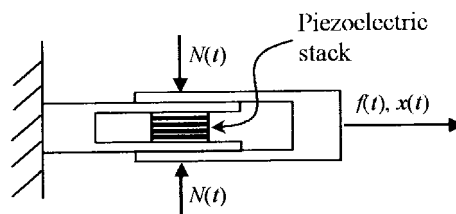


Fig. 1 Schematics of a piezoelectric friction damper (PFD)

connected mechanically in series and electrically in parallel. When they are electrified, the contact force on two friction surfaces can be regulated accordingly due to the electromechanical coupling of piezoelectric materials. The contact force can be determined by

$$N(t) = N_{pre} + \frac{EA d_{33} V(t)}{h} \tag{1}$$

in which N_{pre} is the required pre-load on the stack actuators to avoid any slack in the damper system, E is the Young's Modulus of the PZWT100 material, A is the area of cross section of the stack, h is the thickness of each layer, d_{33} is the piezoelectric strain coefficient and $V(t)$ is the applied voltage on the stack actuators. When $V(t)$ in Eq. (1) is equal to zero, the contact force is constant (N_{pre}) and it corresponds to a passive friction damper. When N_{pre} is negligible, the contact force is proportional to the applied voltage which is fully controllable. The damper in this case is referred to as active friction damper. When both pre-load and voltage are applied, the damper is semi-active and requires less energy in operation. This study is focused on the seismic performance of active friction dampers in suppressing the peak story drift, floor acceleration, base shear and plastic deformation. Note that it is assumed both ends of a stack actuator be fixed and, therefore, the force in each layer is equal to that of the actuator. Additionally, the effect of the hysteresis behavior of a stack piezoelectric actuator on the contact force of a friction damper is neglected for simplicity in this study.

Piezoelectric friction dampers can be installed between a floor of a building structure and the supporting bracket as shown in Fig. 2. To control the structural responses, a damper installed on the structure must deliver an increasing friction force as the slippage in it increases. Additionally, reducing the slipping rate can prevent the built up of excessive slippage. To do so, the friction force of the damper must also increase with the slipping rate. Based on these observations, the voltage signal in Eq. (1) ($N_{pre} = 0$) can be expressed by

$$V(t) = \frac{hN(t)}{EA d_{33}} = \frac{h[e|x(t)| + g|\dot{x}(t)|]}{EA d_{33}} \tag{2}$$

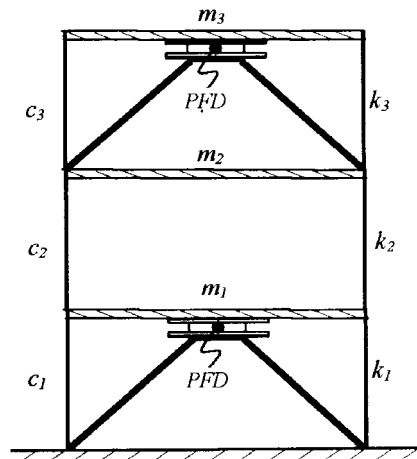


Fig. 2 Installation of dampers on a multi-story building

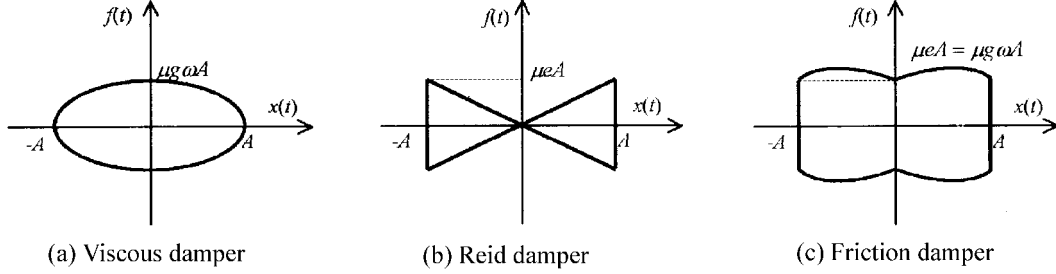


Fig. 3 Hysteresis loops of various dampers

where e and g are the positive gain coefficients, $|x(t)|$ and $|\dot{x}(t)|$ are respectively the absolute values of the slippage and slipping rate of the damper. The friction force of the active damper is thus given by

$$f(t) = \mu N(t) \operatorname{sgn}[\dot{x}(t)] \quad (3)$$

in which μ is the coefficient of friction and $\operatorname{sgn}[\]$ represents the sign of the argument in the bracket. Eqs. (1-3) lead to

$$f(t) = \begin{cases} \mu g \dot{x}(t) + \mu e x(t) & x\dot{x} > 0 \quad (\text{loading}) \\ \mu g \dot{x}(t) - \mu e x(t) & x\dot{x} < 0 \quad (\text{unloading}) \\ -\mu e |x(t)| \leq f(t) \leq \mu e |x(t)| & \dot{x} = 0 \end{cases} \quad (4)$$

The last expression in Eq. (4) represents the stick phase of the friction damper or the change of movement direction. This stick phase is neglected in this study for simplicity. When $e=0$, $f(t) = \mu g \dot{x}(t)$ which represents a viscous damper. When $g=0$, $f(t) = \mu e |x(t)| \operatorname{sgn}[\dot{x}(t)]$, and the active device becomes a non-linear Reid damper (Caughey *et al.* 1970). Therefore, the friction damper with the proposed control logic essentially combines both viscous and non-linear Reid damper mechanisms. When $x(t) = A \sin \omega t$, the corresponding viscous damper has an elliptical hysteresis loop between the friction force and the slippage while the Reid damper shows a triangular loop as presented in Figs. 3(a, b). The hysteresis loop of the friction damper is a combination of the elliptical and triangular loops. Shown in Fig. 3(c) is the case when $e = g\omega$, indicating a nearly rectangular loop. It is thus expected that the proposed control logic performs as effectively as the one recommended by Inaudi (1997). The advantage of the control logic in this study is the inclusion of a velocity sensitive term. This inclusion may make the damper very promising in suppressing the vibration of structures in a velocity-sensitive environment such as high-technology facilities against micro-vibration and civil infrastructure systems under near-fault ground motions.

3. Control design

Numerical simulations on the control effect of dampers on the building's responses are conducted

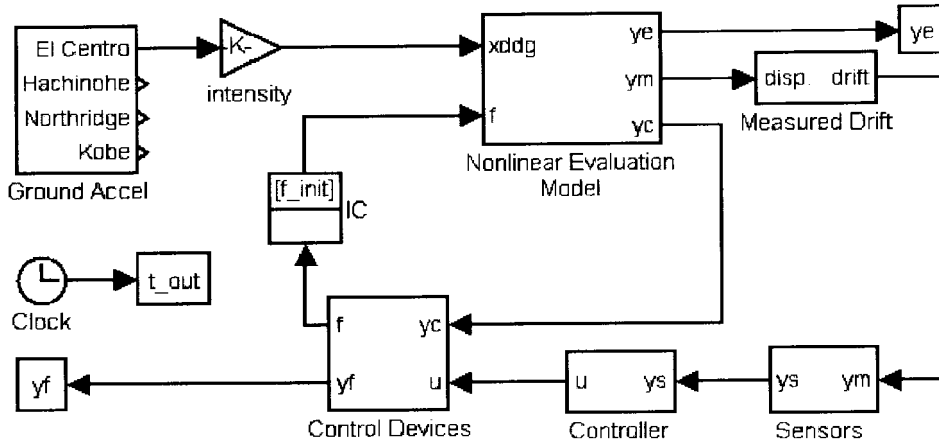


Fig. 4 SIMULINK block diagram for control strategy

using MATLAB software. The closed-loop control strategy is schematically shown in Fig. 4. The Newmark- β method is used to determine the nonlinear responses of the building structure (Ohtori *et al.* 2000). It is implemented in the block called Nonlinear Evaluation Model in Fig. 4. The Model takes various earthquakes of modified intensities, such as 1940 El Centro, 1968 Hachinohe, 1994 Northridge and 1995 Kobe earthquakes, and control forces from the friction damper called Control Devices in Fig. 4. The Model then outputs the structural responses such as relative displacement with respect to the building base and floor acceleration. To simulate the real application, measurement noises are introduced in the Sensors block and, together with the measured responses, they are fed through the Controller block for the determination of the required contact forces. These contact forces are fed back to the Control Devices for the calculation of the required friction forces. Since the friction dampers are operated based on the story drift and the drift rate, a block named Measured Drift is introduced to compute the inter-story drift from the displacements relative to the building base. In addition, an initial condition block IC is used to solve the problem associated with the algebraic loop in the simulation. The simulation time interval is set to be 0.01 sec.

3.1 Sensors

Reliable and inexpensive measurements of inter-story drift can be achieved by using LVDTs (Linear Variable Differential Transformer). LVDTs usually have a natural frequency of at least one order of magnitude over that of the structure. They can be modeled as having a constant magnitude and phase. The sensitivity of the LVDTs used in this study is selected as 10 V/0.08 m based on the maximum uncontrolled structural responses. The measurement noise is modeled as a Gaussian rectangular pulse process with a pulse width of 0.01 seconds and a variance of 0.0003 Volts. Its maximum voltage is approximately 5% of the measured signal for small earthquakes such as 50% El Centro Earthquake. The noise is included in the sensor model. Thus, in term of equations, the sensors can be modeled as

$$y_s = D_s \cdot y_m + v \tag{5}$$

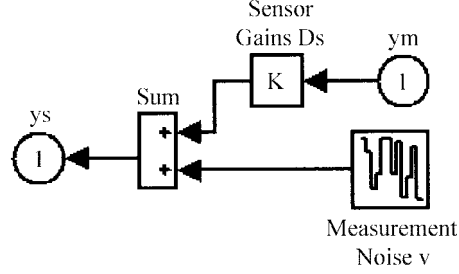


Fig. 5 SIMULINK block diagram for sensors

where y_s is the sensor signal, $D_s = (10/0.08)[I]$ (V/m) is the sensitivity of LVDTs, $y_m = [y_1, y_2 - y_1, \dots, y_{20} - y_{19}]$ is the inter-story drift of the building and v is the noise voltages. The locations of LVDTs are corresponding to the locations of dampers so that a collocated control is implemented. The sensor block shown in Fig. 5 is used to represent the LVDTs.

3.2 Control devices

Piezoelectric actuators can quickly respond to the control voltage signal. Time delay in the piezoelectric friction dampers is very small and thus neglected in this investigation. For the 20-story steel moment-resisting building, each piezoelectric friction damper is designed with a capacity of 93.1 kN based on the current state of practice. It consists of four piezoelectric stacks of 0.0381 m in diameter. Each stack has 24 ceramic disks of 0.508 mm thick. The total height of each stack is approximately 14 mm. The piezoelectric strain coefficient d_{33} is 2.072×10^{-12} m/V. It is considered that the applied voltage $V(t)$ could be as high as 1000 volts. To take into account the flexibility of the damper assemblage, the Young's Modulus E of the PZWT100 material is set to be 86.5% of 4.8×10^{10} N/m² which was provided by the manufacturer. In addition, the pre-load N_{pre} applied on the stack actuators is neglected in the simulation since it is relatively small. Thus the gain factor $K_p (= EAd_{33}/h)$ corresponding to the four piezoelectric stacks is determined to be 133 N/V. The friction coefficient μ is set to 0.35 and the control signal amplifier gain K_a of 100 is used in the simulation.

Dampers can be placed on the structure using a bracing configuration as schematically shown in Fig. 2. The dynamics of the bracing is neglected in this study. Based on the sub-optimal sequential procedure to be discussed in the following section, 80 dampers are optimally distributed from the first to 20th story of the building as [16, 0, 4, 8, 15, 0, 0, 4, 3, 1, 4, 5, 1, 5, 1, 0, 0, 1, 0, 12] with peak acceleration as the objective criterion. For instance, 16 dampers are installed on the first story while 12 dampers are placed on the top story. Multiple dampers installed at the same location are equivalent to a larger damper. In terms of equations, the piezoelectric friction dampers can be modeled as

$$f = K_f \cdot K_t \cdot u, \quad yf = \begin{bmatrix} K_t \cdot u \\ yc \end{bmatrix} \quad (6)$$

where $K_t = \mu \cdot K_p \cdot K_a$ includes the coefficient of friction μ , the piezoelectric stack gain K_p and the gain factor K_a of the control signal amplifier, respectively. K_f is a transformation matrix that

transforms the control force of a single damper installed on each story of the structure into two equal but opposite friction forces applied on each building floor. This matrix accounts for the effect of multiple dampers installed between two adjacent floors. The block diagram in Fig. 6 is used to represent the dampers.

3.3 Digital controller

The control algorithm described in Eq. (3) can be rewritten in the following form:

$$f(k) = \mu g \{ (e/g) |y(k)| \text{sgn}[\dot{y}(k)] + \dot{y}(k) \} \tag{7}$$

where $y(k)$, $\dot{y}(k)$ are the discrete-time inter-story drift and drift rate, respectively. The optimal value of the gain ratio e/g is determined to be $2\omega_0/\pi$ (Chen *et al.* 2000a). The quantity ω_0 denotes the dominant frequency of the uncontrolled displacements of the 20-story building. It was estimated to be 4.731 rad/sec. The gain factor g is set to 3.8×10^5 N-sec/m to ensure that the dampers can generate the maximum friction force nearly equal to their capacity without saturation for 10 earthquake excitations. This algorithm is implemented in the digital controller block shown in Fig. 7. It can be seen from the figure that the inter-story drift was first extracted out from the input sensor

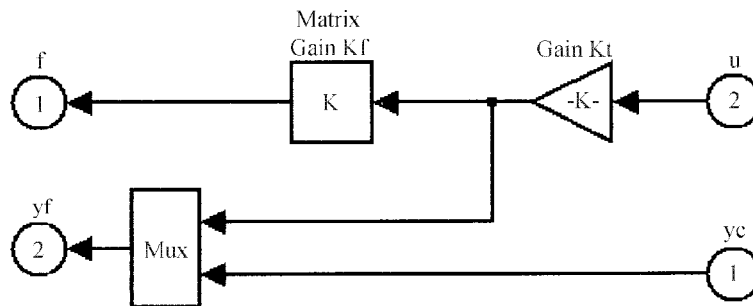


Fig. 6 SIMULINK block diagram for control devices

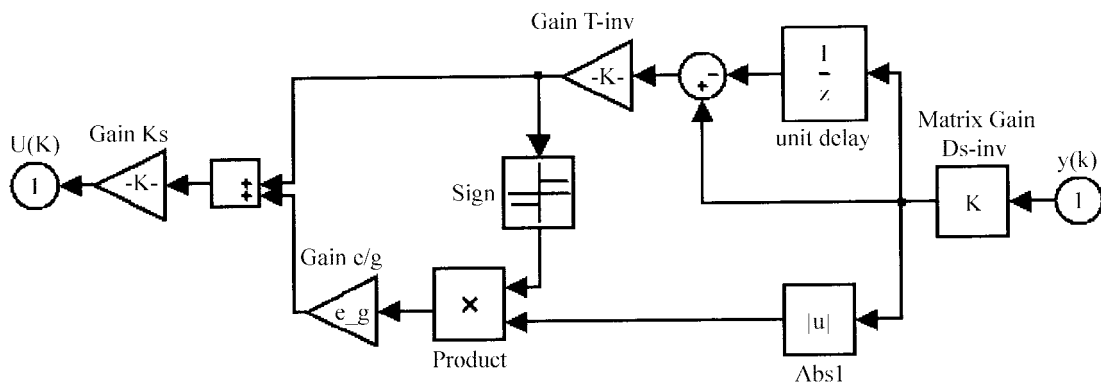


Fig. 7 SIMULINK block diagram for digital controller

signal by multiplying it by a gain matrix Ds^{-1} that is actually the inverse of Ds . A unit delay block is then used to differentiate the drift in order to obtain the drift rate and its sign. The gain T^{-1} is the inverse of the time step 0.01, and the optimal gain ratio e/g is put in the block named Gain e/g . Within the block Gain Ks is a factor equal to the product of g , $1/Ka$ and $1/Kp$, which is used to convert the calculated contact force into control signal $u(k)$ to feed the control device. A/D and D/A converters are included immediately before and after the digital controller block to convert from analog to digital signal, and vice versa.

Because the drift rate is obtained by differentiating the feedback drift, any saturation of sensors will lead to the loss of the drift rate information. Under these circumstances, the control force is equal to zero. Therefore, the sensitivity of LVDTs must be determined based on the maximum peak drift of uncontrolled building structures. For the 20-story building under consideration, its maximum peak drift is 0.075 m induced by Kobe Earthquake. A sensitivity of 10 V/0.08 m was used in this study.

4. Sub-optimal placement of dampers and objective criterion

It is believed that certain structural locations are advantageous for actuator placement (Cheng *et al.* 1988). To place piezoelectric friction dampers on a structure to efficiently mitigate its earthquake-induced responses, two aspects need to be investigated. First, a practical yet effective procedure must be developed for the placement of dampers on the structure. The damper placement is a combinatorial optimization problem since the design space is discrete. Theoretically, it is possible to consider all combinations of damper locations. However, it is time-consuming due to an exceptionally large number of combinations and becomes impractical for high-rise buildings. No efficient algorithm can solve the general problem of optimal damper placement (Lu *et al.* 1994). In this study, a sub-optimal procedure is employed to sequentially place dampers on the structure one by one. At each step, a damper is considered on all possible locations of the 20-story building and the reduction in an objective criterion is calculated. The damper is then placed at the location corresponding to the maximum reduction in the objective criterion. The same process is repeated until the required numbers of dampers have been placed on the structure or the structural responses are reduced by a predetermined percentage. In this paper, the former criterion is used. It is noted that sometimes, adding one damper cannot further suppress the responses based on the criterion and, in this case, two or more dampers should be placed on the structure simultaneously.

Second, an optimization objective must be established in order to achieve certain design goals. Peak acceleration and peak drift ratio are two important parameters in building designs. They are considered here as objective candidates for determining the damper profile along the structure height. In addition, damper placement is not only dependent on the structural properties, but is also related to the characteristics of earthquake excitations. Four inputs: 150% El Centro, 150% Hachinohe, 100% Northridge and 100% Kobe Earthquake, are used to determine the locations of 80 dampers sequentially on the 20-story benchmark building based on the maximum reduction in peak acceleration. Their corresponding damper profiles are referred to as Profile3a, Profile6a, Profile8a and Profile10a. For each profile, the peak floor acceleration is computed for all 10 earthquake inputs and they are listed in Table 1 after normalized by the uncontrolled peak acceleration. The statistical characteristics of the 10 normalized accelerations are given at the bottom of the table. It can be observed from the statistical results that Profile8a has the lowest maximum acceleration ratio and

Table 1 Peak floor acceleration normalized by uncontrolled response (Based on acceleration criterion with 80 dampers)

Damper profile		Profile			
		Profile3a	Profile6a	Profile8a	Profile10a
Earthquake inputs					
50% El Centro		0.796	0.839	0.838	0.846
100% El Centro		0.740	0.831	0.817	0.837
150% El Centro		0.741	0.853	0.837	0.857
50% Hachinohe		1.054	0.869	0.889	0.893
100% Hachinohe		0.903	0.862	0.867	0.888
150% Hachinohe		0.976	0.889	0.923	0.928
50% Northridge		0.939	0.951	0.944	0.967
100% Northridge		0.910	0.989	0.869	0.975
50% Kobe		0.778	0.805	0.826	0.828
100% Kobe		0.865	0.902	0.911	0.875
max(x)		1.054	0.989	0.944	0.975
$\bar{x} = \text{mean}(x)$		0.870	0.879	0.872	0.889
$\sum_{i=1}^{10} (x_i - \bar{x})^2$		0.1001	0.0283	0.0171	0.0243

Table 2 Peak drift ratio normalized by uncontrolled response (Based on drift criterion with 80 dampers)

Damper profile		Profile			
		Profile3d	Profile6d	Profile8d	Profile10d
Earthquake inputs					
50% El Centro		0.779	0.795	0.803	0.829
100% El Centro		0.775	0.792	0.799	0.828
150% El Centro		0.773	0.796	0.798	0.826
50% Hachinohe		0.915	0.903	0.915	0.911
100% Hachinohe		0.919	0.897	0.915	0.909
150% Hachinohe		0.934	0.912	0.938	0.927
50% Northridge		0.918	0.905	0.922	0.919
100% Northridge		0.931	0.926	0.895	0.925
50% Kobe		0.916	0.884	0.888	0.918
100% Kobe		0.762	0.718	0.745	0.698
max(x)		0.934	0.926	0.938	0.927
$\bar{x} = \text{mean}(x)$		0.862	0.853	0.862	0.869
$\sum_{i=1}^{10} (x_i - \bar{x})^2$		0.0544	0.0455	0.0420	0.0491

standard deviation, indicating more consistent performance for various earthquakes. This damper profile is thus recommended for acceleration control of the 20-story building even though the mean normalized acceleration associated with the damper distribution is slightly larger than that from Profile3a.

Similarly, the maximum story drift-over-height ratio is used as a criterion. Based on this criterion,

four damper profiles: Profile3d, Profile6d, Profile8d and Profile10d can be obtained. For each damper profile, the peak drift ratio normalized by their corresponding uncontrolled quantity is given in Table 2 under all 10 earthquake inputs. The statistical characteristics, also listed in Table 2, indicate that Profile6d has marginally better overall performance in reducing the drift ratio of the structure.

To determine whether peak acceleration or peak inter-story drift ratio should be used as a criterion for damper placement, their reduction are presented in Figs. 8(a, b) as the number of dampers on the structure increases. The heavy solid line represents that dampers are placed on the structure based on maximum reduction in peak acceleration of the structure subjected to the 100% Northridge Earthquake. The light solid line represents that dampers are placed on the structure based on maximum reduction in peak story drift ratio when the building structure is excited by 150% Hachinohe Earthquake. It can be observed from Fig. 8 that use of the peak acceleration as an optimization criterion results in significant reduction in both peak acceleration and peak inter-story drift ratio. On the other hand, if peak inter-story drift ratio is used as the criterion, the reduction in peak acceleration remains almost unchanged after 10 dampers have been installed on the structure. Therefore, the damper distribution based on Profile8a: [16, 0, 4, 8, 15, 0, 0, 4, 3, 1, 4, 5, 1, 5, 1, 0, 0, 1, 0, 12], is finally employed in this study.

To further understand the effect of earthquake characteristics on the optimal distribution of various number of dampers, Table 3 gives the statistical results of acceleration reduction with 20, 50, 80, and 137 dampers respectively placed on the structure under four earthquake inputs. It can be seen from the table that, regardless of the number of dampers, the profiles determined under the excitation of 100% Northridge Earthquake are generally superior to others in reducing the peak acceleration of the structure subjected to all 10 earthquake inputs. In addition, as the number of dampers increases, the overall maximum structural responses corresponding to the 150% El Centro (0.523 g) and 150% Hachinohe (0.344 g) Earthquakes increase, while those corresponding to the 100% Northridge (0.843 g) and 100% Kobe (0.590 g) Earthquakes generally decrease. This result indicates that placing dampers on various floors of a structure based on impulsive types of strong

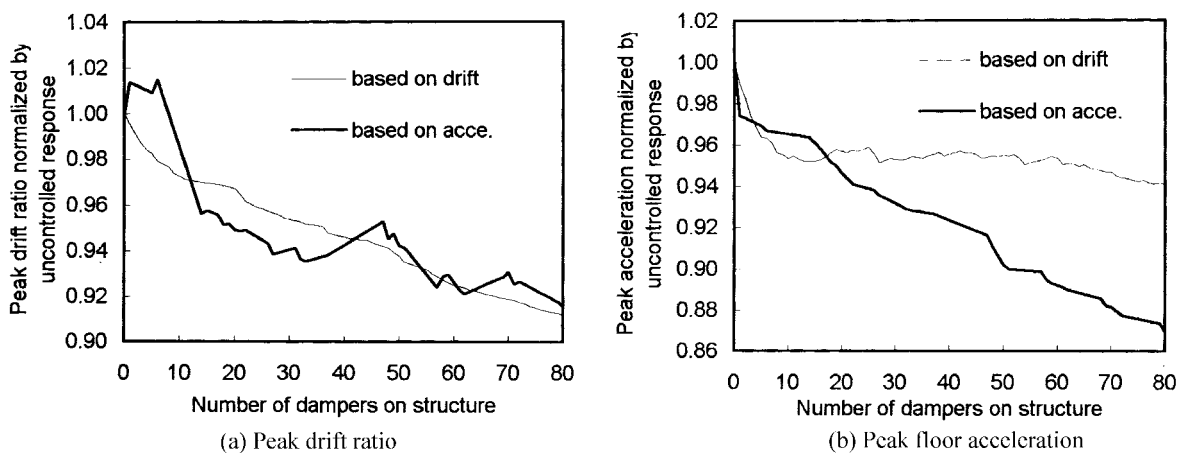


Fig. 8 Performance of acceleration- and drift-based criteria

Table 3 Statistical characteristics for different damper profile (Based on acceleration criterion with 20, 50, 80 or 137 dampers)

Damper profiles		Profile3a El Centro (150%)	Profile6a Hachinohe (150%)	Profile8a Northridge (100%)	Profile10a Kobe (100%)
20	$\max(x)$	0.977	0.981	0.985	1.011
	\bar{x}	0.935	0.945	0.935	0.973
	$\sum_{i=1}^{10} (x_i - \bar{x})^2$	0.0101	0.0042	0.0078	0.0044
50	$\max(x)$	1.040	0.988	0.959	1.006
	\bar{x}	0.915	0.914	0.897	0.918
	$\sum_{i=1}^{10} (x_i - \bar{x})^2$	0.0754	0.0157	0.0113	0.0205
80	$\max(x)$	1.054	0.989	0.944	0.975
	\bar{x}	0.870	0.879	0.872	0.889
	$\sum_{i=1}^{10} (x_i - \bar{x})^2$	0.1001	0.0283	0.0171	0.0243
137	$\max(x)$	1.178	1.141	0.914	0.998
	\bar{x}	0.880	0.870	0.824	0.837
	$\sum_{i=1}^{10} (x_i - \bar{x})^2$	0.2789	0.1418	0.0394	0.1014

earthquake inputs such as Northridge and Kobe lead to better performance of the controlled structure under general earthquake excitations.

5. Simulation and evaluation of the control strategy

The optimal damper distribution, Profile8a, was considered for the evaluation of seismic effectiveness of active dampers. When 80 dampers were placed on the 20-story building, the time histories of acceleration and drift responses at the top story are given in Figs. 9-12 for controlled and uncontrolled structures, together with the maximum absolute acceleration and maximum drift ratio profiles along the height of the building. Figs. 9-12 also show the control force vs. drift ratio curve for one damper located at the top story of the building. Only the responses for four earthquake inputs are presented. For comparison purposes, similar structural response curves are presented in Figs. 13 and 14 when 137 dampers were installed and distributed on the structure as [13, 11, 5, 0, 2, 1, 3, 6, 0, 4, 10, 4, 1, 8, 11, 4, 9, 12, 0, 33]. In all the figures, the light line represents the response of uncontrolled structure while the heavy line denotes the response of the structure controlled with active dampers.

It can be seen from the response time histories that use of the active dampers does not alter the phase information of the responses but significantly suppresses their peak values. Therefore, the control strategy increases the damping of the building structure. Of particular interest is the plastic

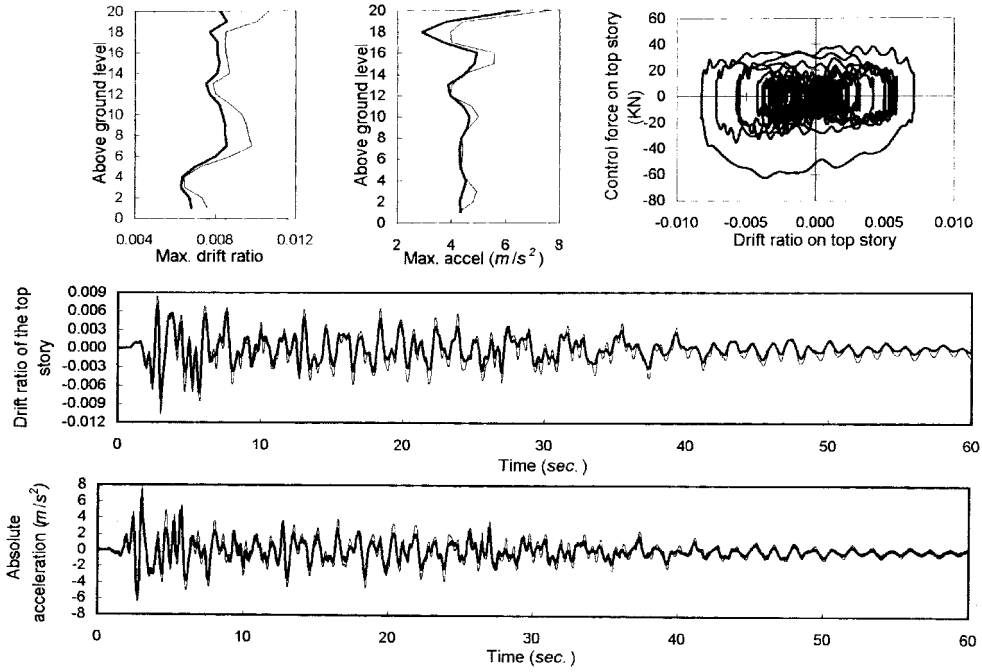


Fig. 9 Uncontrolled responses (light line) vs. controlled responses (heavy line) with 80 dampers under 150% El Centro Earthquake

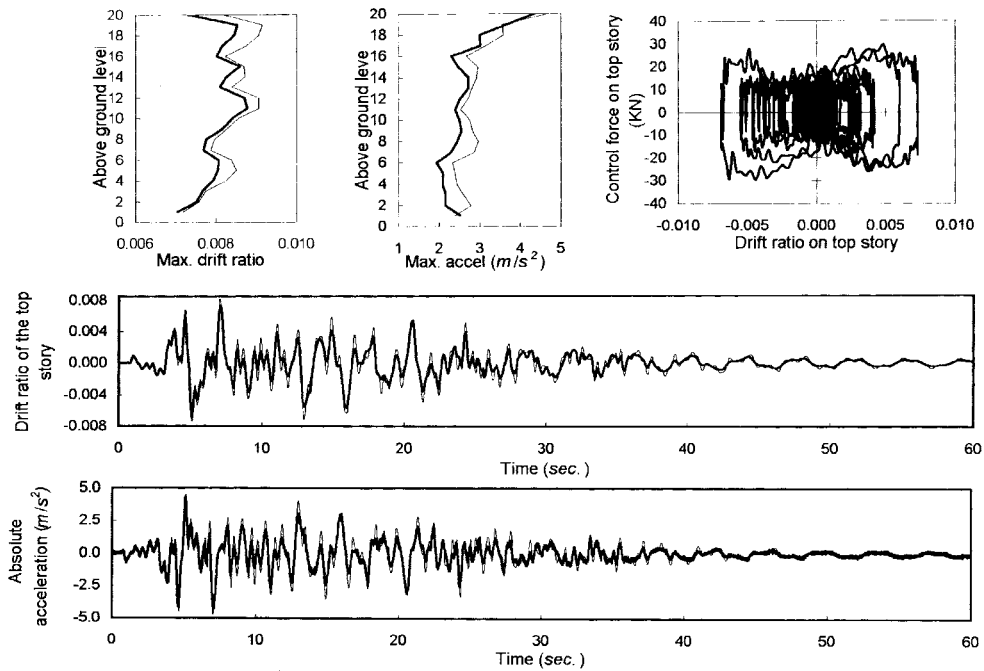


Fig. 10 Uncontrolled responses (light line) vs. controlled responses (heavy line) with 80 dampers under 150% Hachinohe Earthquake

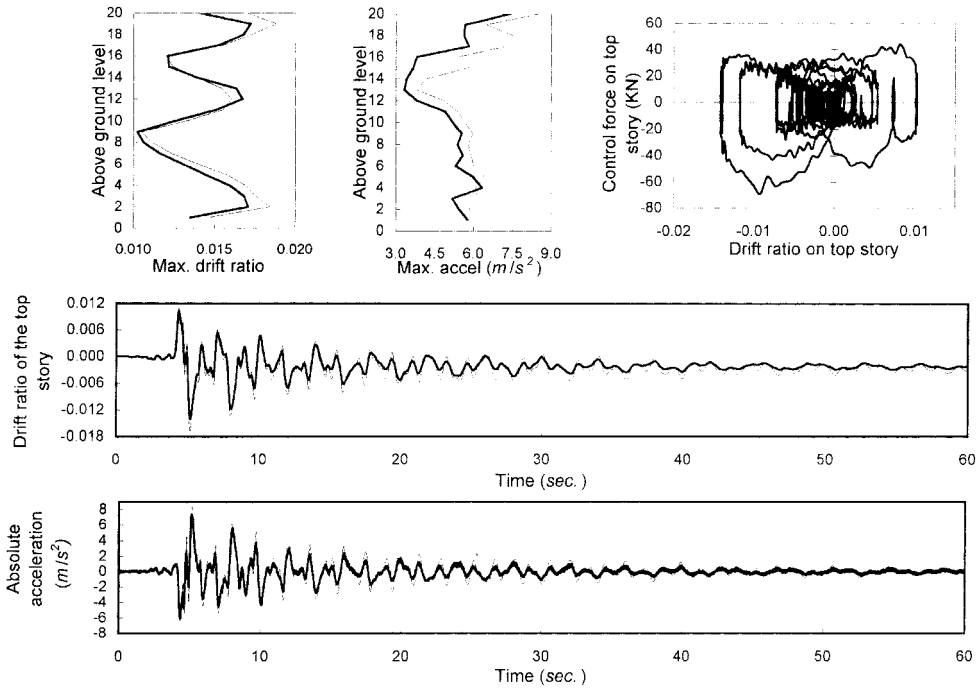


Fig. 11 Uncontrolled responses (light line) vs. controlled responses (heavy line) with 80 dampers under 100% Northridge Earthquake

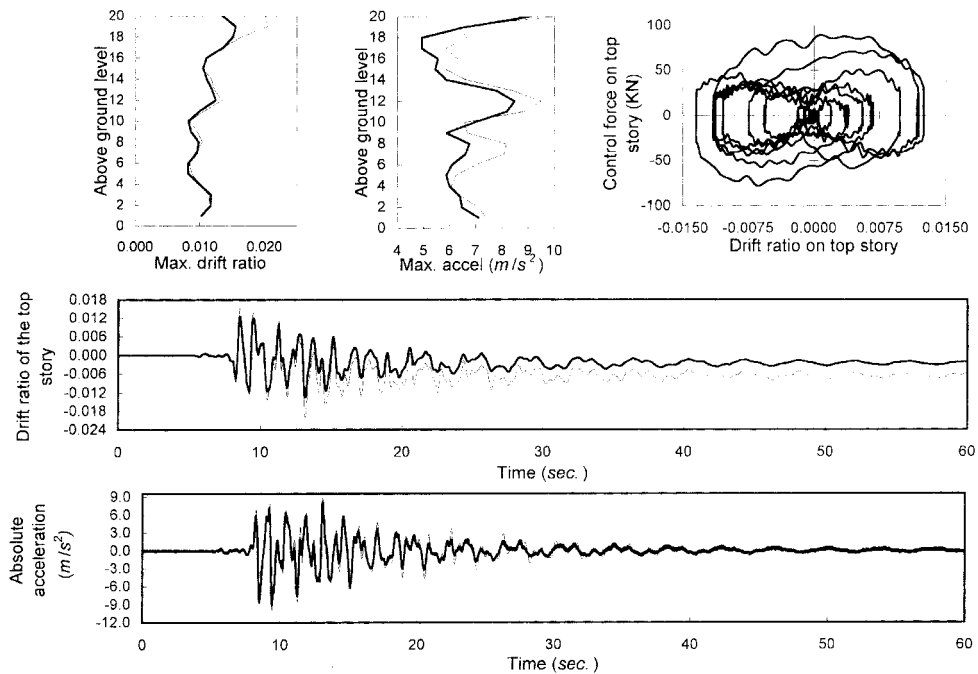


Fig. 12 Uncontrolled responses (light line) vs. controlled responses (heavy line) with 80 dampers under 100% Kobe Earthquake

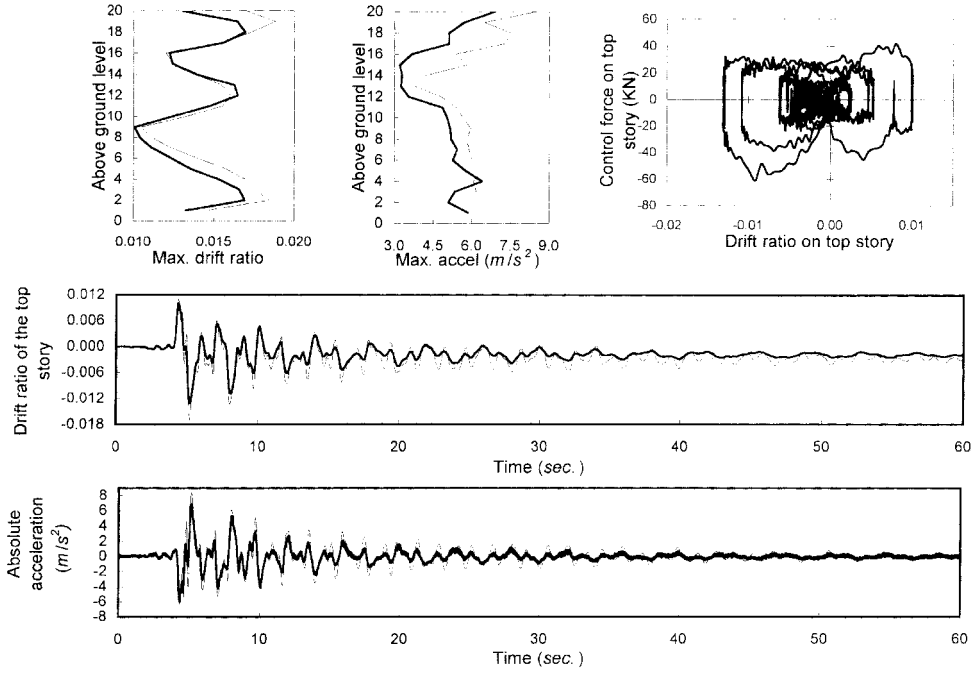


Fig. 13 Uncontrolled responses (light line) vs. controlled responses (heavy line) with 137 dampers under 100% Northridge Earthquake

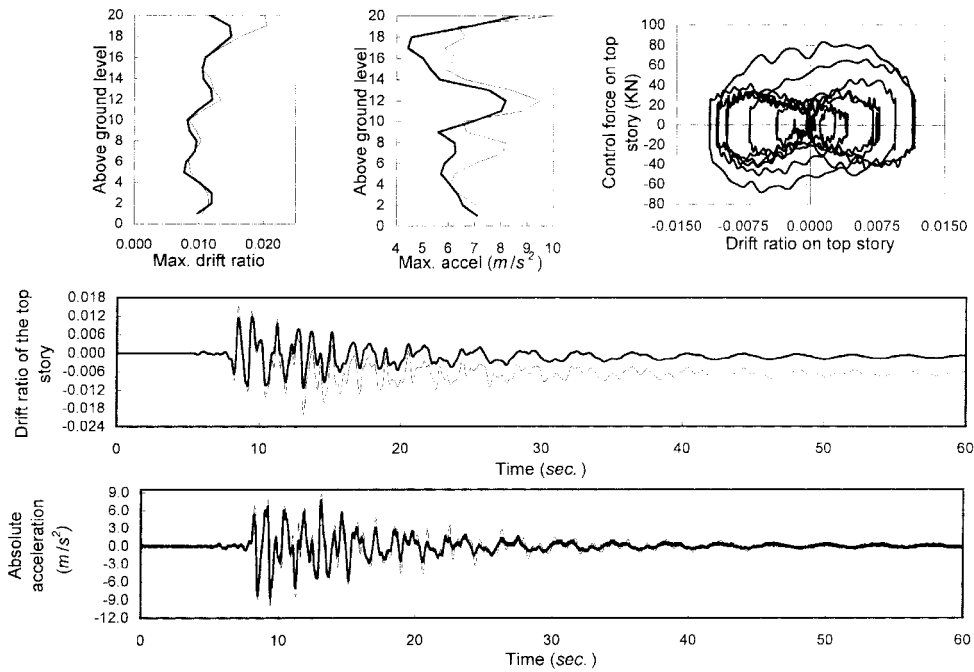


Fig. 14 Uncontrolled responses (light line) vs. controlled responses (heavy line) with 137 dampers under 100% Kobe Earthquake

deformation in column under the Kobe Earthquake. Shown in Figs. 12 and 14, the plastic deformation is represented by the amount of permanent drift at the end of the earthquake excitation. It is substantially reduced with the introduction of active piezoelectric friction dampers. The maximum story drift-to-height ratios become more uniformly distributed along the height of the 20-story building due to the effect of dampers. The overall maximum acceleration always occurs at the top of the building while the location corresponding to overall maximum story drift ratio may vary from one case to another. All cases show a nearly rectangular force-drift loop for every damper, indicating the desired energy dissipation capability.

In comparison with Figs. 11 and 12, Figs. 13 and 14 indicates that, under the same earthquake input, the maximum control force generated by one damper when 137 dampers was installed on the structure is quite smaller than that when 80 dampers was used. This result means that dampers in the 137-damper profile are not as efficient as those in the 80-damper profile. The main reason is that the same gain factor $g = 3.8 \times 10^5$ N-sec/m is employed for these two damper profiles. In general, more dampers mean larger reduction in structural responses. Since the control force generated by each damper is proportional to the structural responses, a relatively larger gain factor g is needed to maintain the damper efficiency while more dampers are placed on the structure. However, continually increasing the gain factor may result in saturation of the control device. Therefore, it is essential to select an appropriate gain factor for the efficient control of structures with active dampers. Table 4 lists the maximum control force of all dampers and the associated story drift-to-height ratio and maximum floor acceleration as a function of the gain factor. It can be observed from the table that both drift ratio and floor acceleration decrease as the gain factor increases up to 5.0×10^5 N-sec/m. Beyond that point, control devices are saturated and the floor acceleration increases. Although the drift ratio continues to decrease slightly, the overall performance of dampers somewhat degrades. For practical application, it is recommended that the gain factor be selected such that the maximum control force of dampers under the design earthquakes is approximately equal to 90% capacity of the dampers. The remaining capacity (10%) is reserved to accommodate extreme events beyond the design earthquakes. Based on the above criterion, a gain factor of 4.5×10^5 N-sec/m can be used for the design of 137 dampers as Table 4 indicates that its corresponding control force is 88% of the damper's capacity.

The maximum story drift-to-height ratio, the maximum floor acceleration, the maximum base shear, the displacement ductility and control force are critical parameters for design of the building

Table 4 Maximum structural responses and control forces with different gain values (137-damper profile, 100% Kobe Earthquake)

Gain factor g	Max. control force (kN)	Max. drift ratio	Max. acceleration (m/s^2)
0	0	0.0201	9.974
3.8×10^5	82.98	0.0150	8.627
4.5×10^5	81.58	0.0142	8.245
5.0×10^5	89.57	0.0138	8.155
5.5×10^5	93.1(3)*	0.0136	8.170
6.0×10^5	93.1(3)*	0.0136	8.292
6.5×10^5	93.1(4)*	0.0133	8.457

*The value in parenthesis represents the number of locations with saturated control devices.

Table 5 Effectiveness of the proposed control strategy (80 dampers)

Earthquake (Intensity)	El Centro (0.5/1.0/1.5)	Hachinohe (0.5/1.0/1.5)	Northridge (0.5/1.0)	Kobe (0.5/1.0)	Max. Value
Max. Drift Ratio*	0.814	0.925	0.935	0.925	0.957
	0.810	0.927	0.916	0.757	
	0.805	0.957			
Max. Floor Accel.*	0.838	0.889	0.944	0.826	0.944
	0.817	0.867	0.869	0.911	
	0.837	0.923			
Max. Base Shear*	0.870	1.015	0.933	1.012	1.053
	0.864	0.996	1.015	1.053	
	0.963	1.028			
Displacement Ductility*	0.863	0.966	0.891	0.945	0.966
	0.859	0.961	0.933	0.699	
	0.818	0.930			
Control Force (kN)	23.184	16.169	48.521	50.508	88.838
	42.632	24.664	68.922	88.838	
	62.258	33.668			

*Normalized by uncontrolled structure responses.

Table 6 Effectiveness of the proposed control strategy (137 dampers)

Earthquake (Intensity)	El Centro (0.5/1.0/1.5)	Hachinohe (0.5/1.0/1.5)	Northridge (0.5/1.0)	Kobe (0.5/1.0)	Max. Value
Max. Drift Ratio*	0.777	0.908	0.907	0.882	0.933
	0.771	0.908	0.900	0.731	
	0.772	0.933			
Max. Floor Accel.*	0.765	0.884	0.914	0.793	0.914
	0.735	0.812	0.809	0.865	
	0.749	0.911			
Max. Base Shear*	0.839	1.041	0.914	1.010	1.083
	0.816	1.011	1.027	1.083	
	0.932	1.040			
Displacement Ductility*	0.819	0.948	0.853	0.883	0.948
	0.812	0.941	0.923	0.694	
	0.776	0.905			
Control Force (kN)	21.255	16.101	42.910	48.226	82.979
	38.754	24.079	62.554	82.979	
	56.286	32.733			

*Normalized by uncontrolled structure responses.

structure and control system. They are presented in Table 5 for the 80-damper profile and Table 6 for the 137-damper profile. Both cases use the gain factor (g) equal to 3.8×10^5 N-sec/m. These tables clearly show that both the story drift ratio and floor acceleration are significantly mitigated.

The maximum drift ratio of the 20-story building could be reduced by 26.9% under the 1995 Kobe Earthquake when 137 dampers are employed. The maximum floor acceleration could be suppressed by 26.5% under the 1940 El Centro Earthquake. However, the reduction in base shear is much smaller and in several cases, the base shear is even slightly increased as a result of installation of the dampers on the structure. This effect is likely caused by the local acceleration jumping corresponding to the change in direction of dampers movement (Chen *et al.* 2000a). Due to presence of the dampers, the ductility demand on various columns is substantially relieved. For instance, the ductility reduction is over 30% under the 1995 Kobe Earthquake. This result indicates significant reduction in damage of steel columns during strong earthquakes.

6. Conclusions

A recently proposed control logic has been employed to drive active piezoelectric friction dampers. It combines the mechanisms of a non-linear Reid damper and a viscous damper, and generates a nearly rectangular force-displacement hysteresis loop with an optimal gain ratio (e/g) proportional to the dominant frequency of the uncontrolled structural responses. Therefore, active dampers driven by the control logic can dissipate a significant amount of energy when installed on a structure subjected to dynamic loading.

A sequential procedure was developed to sub-optimally place dampers on a 20-story building. The damper distribution along the height of the building based on peak acceleration reduction rather than peak story drift-to-height ratio as an optimization criterion renders superior performance. In addition, impulsive types of strong earthquake inputs such as near-fault records should be used in the determination of optimal placement of dampers for overall performance of the building under various earthquake excitations. It is recommended that the gain factor (g), which is associated with the viscous damper, be selected such that the maximum control force of dampers is approximately equal to 90% of the dampers' capacity to avoid the adverse effect of saturation in control devices.

The proposed control logic and active dampers can effectively suppress the peak responses of the building by adding supplemental damping. Both the maximum acceleration and story drift ratio can be reduced up to 27% with 137 dampers installed on the structure. The ductility demand, an indication of damage, can be mitigated by 30%. The control force required to achieve the above performance is within the capacity of a practical damper and thus the proposed control strategy has potential to be implemented in real structures.

Acknowledgements

This study was sponsored by the U.S. National Science Foundation under Grant No. CMS-9733123 with Drs. S.C. Liu and P. Chang as Program Directors. The results, opinions and conclusions expressed in this paper are solely those of the authors and do not necessarily represent those of the sponsor. The authors would like to extend their sincere thanks to Professor B.F. Spencer, Jr. from the University of Notre Dame for making the MATLAB-based computer program available for this study.

References

- Caughey, T.K. and Vijayaraghavan, A. (1970), "Free and forced oscillations of a dynamic system with linear hysteretic damping (non-linear theory)", *Int. J. Non-Linear Mech.*, **5**, 533-555.
- Chen, G.D. and Chen, C.C. (2000a), "Behavior of piezoelectric friction dampers under dynamic loading", *Proc. SPIE Symposium on Smart Structures and Materials: Smart Systems for Bridges, Structures, and Highways*, Newport Beach, CA, **3988**, 54-63.
- Chen, G.D., Wu, J. and Garrett (2000b), "Preliminary design of piezoelectric friction dampers for reducing the seismic responses of structures", *Proceedings of the 14th ASCE Engineering Mechanics Conference*, Austin, Texas, May 21-24.
- Chen, G.D. and Wu, J. (2001), "Optimal placement of multiple tuned mass dampers for seismic structures", *J. Struct. Eng.*, ASCE, **127**, 1054-1062.
- Cheng, F.Y. and Pantelides, C.P. (1988), "Optimal placement of actuators for structural control", *Technical Report NCEER-88-0037*, August 15.
- Housner, G.W., Soong, T.T. and Masri, S.F. (1994), "Second generation of active structural control in civil engineering", *Proc. 1st World Conf. Struct. Control*, Los Angeles, CA, Panel: 3-18.
- Inaudi, J.A. (1997), "Modulated homogeneous friction: a semi-active damping strategy", *Earthq. Engrg. Struct. Dyn.*, **26**, 361-376.
- Kamada, T., Fujita, T., Hatayama, T., Arikabe, T., Murai, N., Aizawa, S. and Tohyama, K. (1998), "Active vibration control of flexural-shear type frame structures with smart structures using piezoelectric actuators", *Smart Mater. Struct.*, **7**, 479-488.
- Kannan, S., Uras, H.M. and Aktan, H.M. (1995), "Active control of building seismic response by energy dissipation", *Earthq. Engrg. Struct. Dyn.*, **24**, 747-759.
- Lu, J., Thorp, J.S., Aubert, B.H. and Larson, L.B. (1994), "Optimal tendon configuration of a tendon control system for a flexible structure", *J. Guidance, Control and Dynamics*, **17**, 161-169.
- Ohtori, Y., Christenson, R.E. and Spencer, Jr., B.F. (2000), "Benchmark control problems for seismically excited nonlinear buildings", <http://www.nd.edu/~quake/nlbench.html>.
- Yang, C. and Lu, L.W. (1994), "Seismic response control of cable-stayed bridges by semi-active friction damping", *Proc. U.S. National Conf. Earthquake Engrg.*, **1**, Chicago, 911-920.